Recent advances in the Virtual Fields Method for Nonlinear Elasticity

Prof. Stéphane AVRIL

MINES Saint-Étienne
Une école de l'IMT
UNIVERSITÉ DE LYON
Inserm
Institut national de la santé et de la recherche médicale
SAINBIOSE
SAnté INgéniérie BIOlogie Saint-Etienne
U1059 • INSERM • SAINT-ETIENNE

OUTLINE

I. Introduction and state of the art of the VFM

II. Recent developments and generalized VFM

III. New applications in progress

avril@emse.fr

Introduction and state of the art of the VFM

1. Soft tissue mechanics

2. Stiffness reconstruction in arterial lesions

3. The basic VFM

avril@emse.fr

Soft biological tissues: many challenges for continuum mechanics

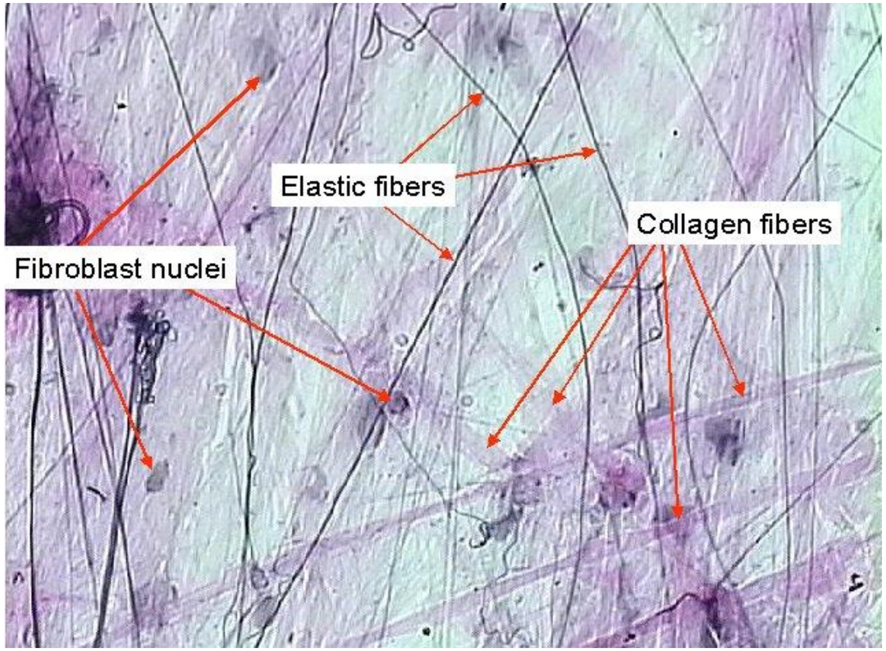

Hyperelasticity of Soft Tissues and Related Inverse Problems. Stéphane Avril, Sam Evans
Material Parameter Identification and Inverse Problems in Soft Tissue Biomechanics, 573, Springer, pp.37 - 66, 2016,

MOTIVATION

Most of my research tries to decipher the regulation and spatial distribution of mechanical properties in soft tissues by:

- ❑ Developing methodologies to identify the mechanical properties of soft tissues
- ❑ Developing models to predict the evolution of these mechanical properties with disease and age

avril@emse.fr

Hyperelasticity

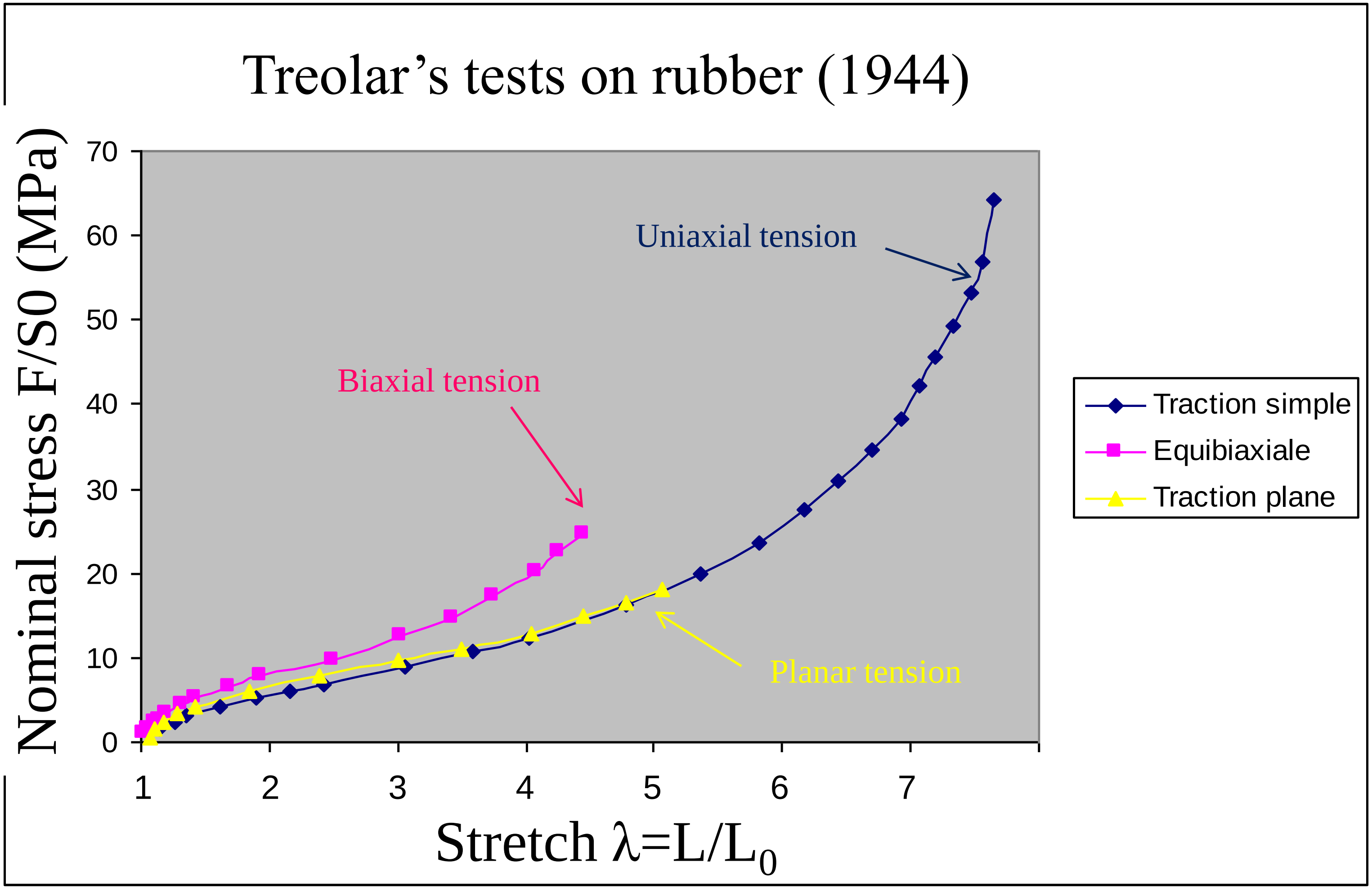

avril@emse.fr

MINES Saint-Étienne

Strain energy density

Stored energy per unit volume

$$\frac{1}{A_0 L_0}\int F\dot{L}dt = \int S\dot{\lambda}dt$$

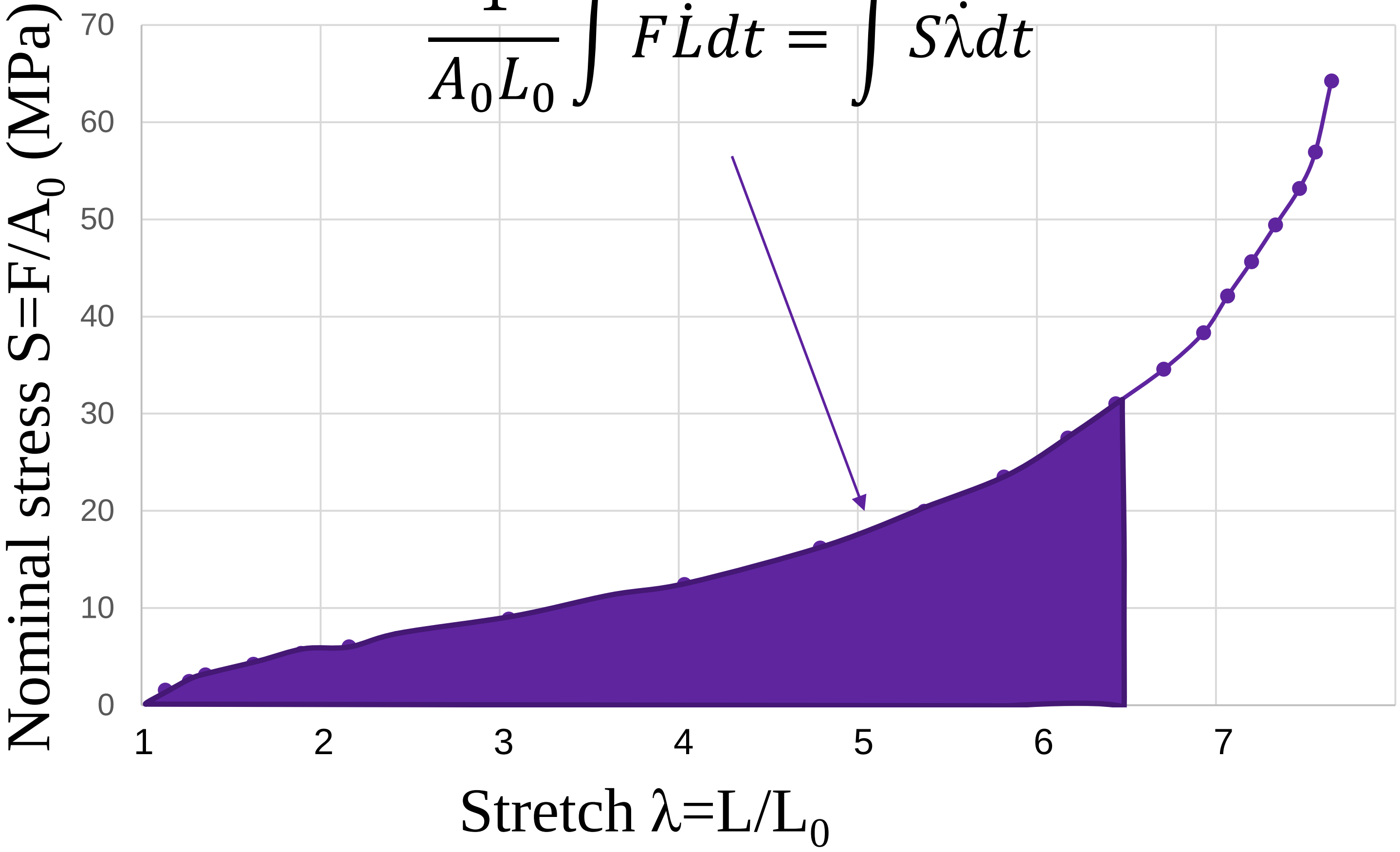

Hyperelasticity

Stored energy per unit volume

$$\int \boldsymbol{S} : \dot{\mathbf{F}} dt = \int \boldsymbol{\pi} : \dot{\mathbf{E}} dt = \Psi(\mathbf{E})$$

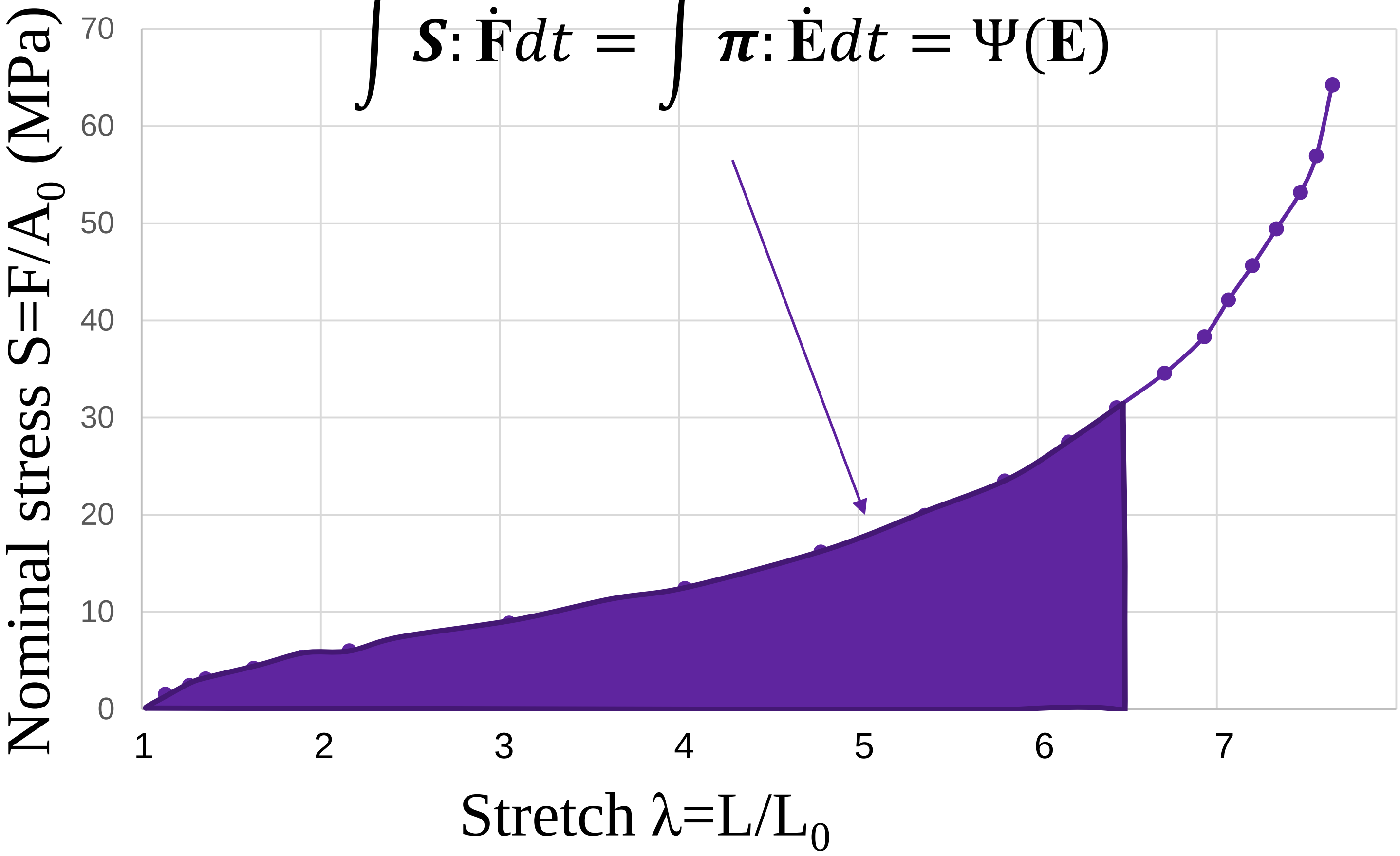

avril@emse.fr

MINES Saint-Étienne

compressible hyperelastic behaviour

$$\boldsymbol{\sigma} = J\mathbf{F}.\frac{\partial \Psi}{\partial \mathbf{E}}.\mathbf{F}^T$$

incompressible hyperelastic behaviour (J=1)

$$\boldsymbol{\sigma} = \mathbf{F}.\frac{\partial \Psi}{\partial \mathbf{E}}.\mathbf{F}^T + c\mathbf{I}$$

Strain energy density:

$$\Psi = ?$$

Anisotropic strain energy density

$$\Psi_f(I_4, I_6) = \frac{k_1}{2k_2} \sum_{i=4,6} \{exp[k_2(I_i - 1)^2] - 1\},$$

(Holzapfel et al., 2000)

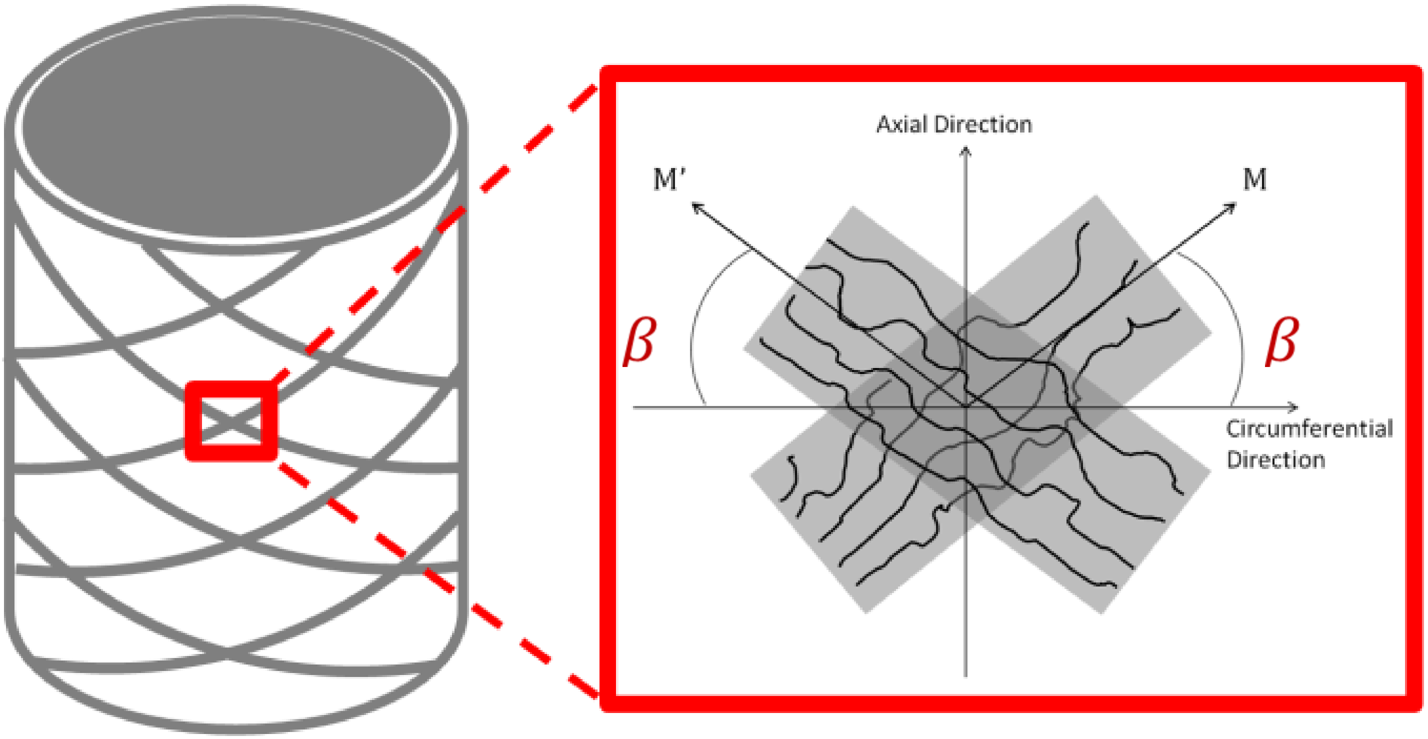

PARAMETERS TO BE IDENTIFIED

Strain energy functions:

$$\Psi(\mathbf{E}) = \phi^{e} W^{e}(\mathbf{F}^{e}) + \phi^{m} W^{m}(\lambda^{m}) + \sum_{j=1}^{4} \phi^{c_j} W^{c_j}(\lambda^{c_j})$$

$$W^{e}(\mathbf{F}^{e}) = \frac{c^{e}}{2}\left[\mathrm{tr}\left((\mathbf{F}^{e})^{T}\mathbf{F}^{e}\right) - 3\right]$$

$$W^{m}(\lambda^{m}) = \frac{c_2^{m}}{4c_3^{m}}\left[e^{c_3^{m}((\lambda^{m})^2-1)^2} - 1\right]$$

$$W^{c}(\lambda^{c_j}) = \frac{c_2^{c}}{4c_3^{c}}\left[e^{c_3^{c}((\lambda^{c_j})^2-1)^2} - 1\right]$$

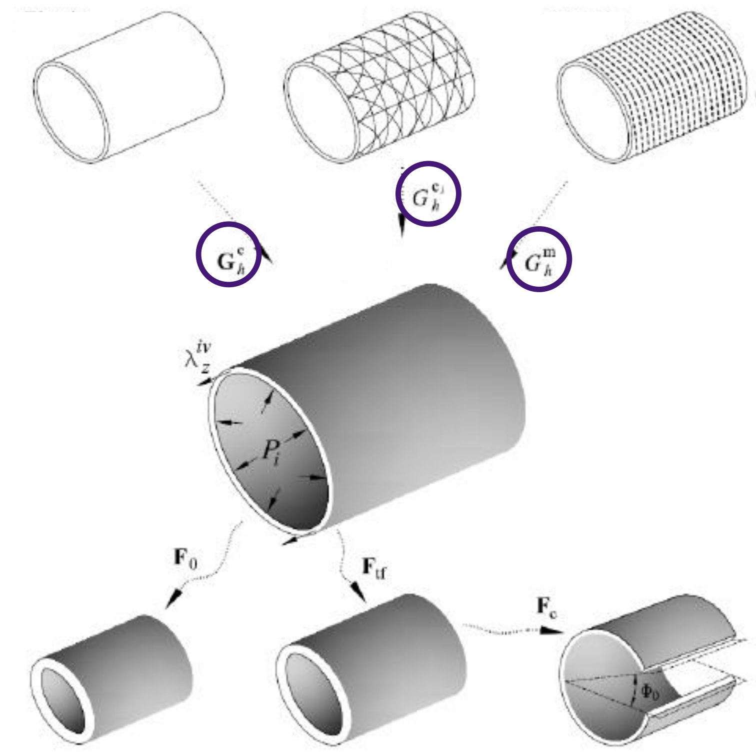

avril@emse.fr

MINES Saint-Étienne

Full-field strain measurement across the outer surface of the artery

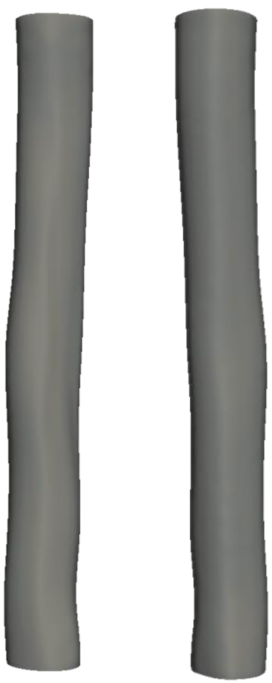

Posterior Anterior

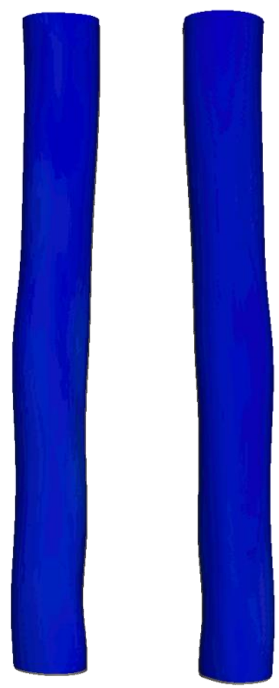

Posterior Anterior

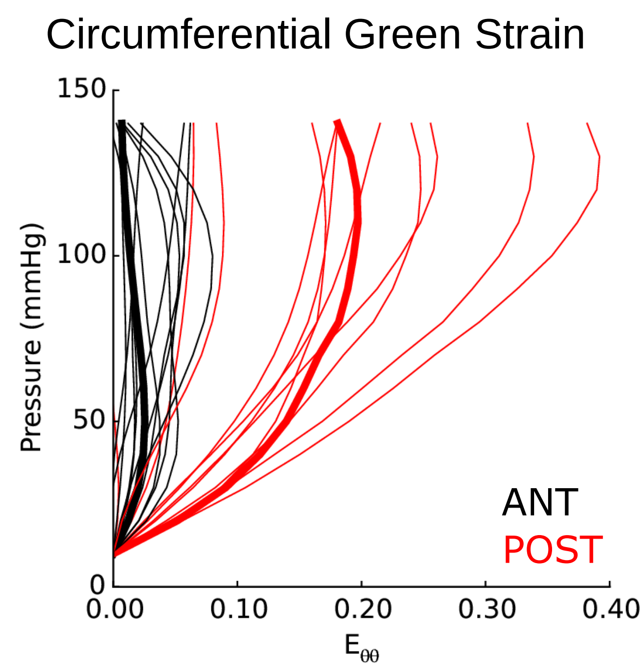

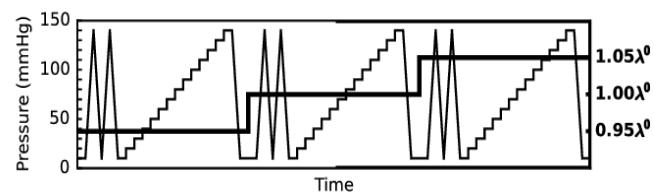

Bersi et al, Biomechanics and modeling in mechanobiology 18 (1), 203-218
Bersi et al, Journal of biomechanical engineering 138 (7), 071005

Obtained linearized circumferential stiffness

Bersi et al, Scientific reports 10 (1), 1-23

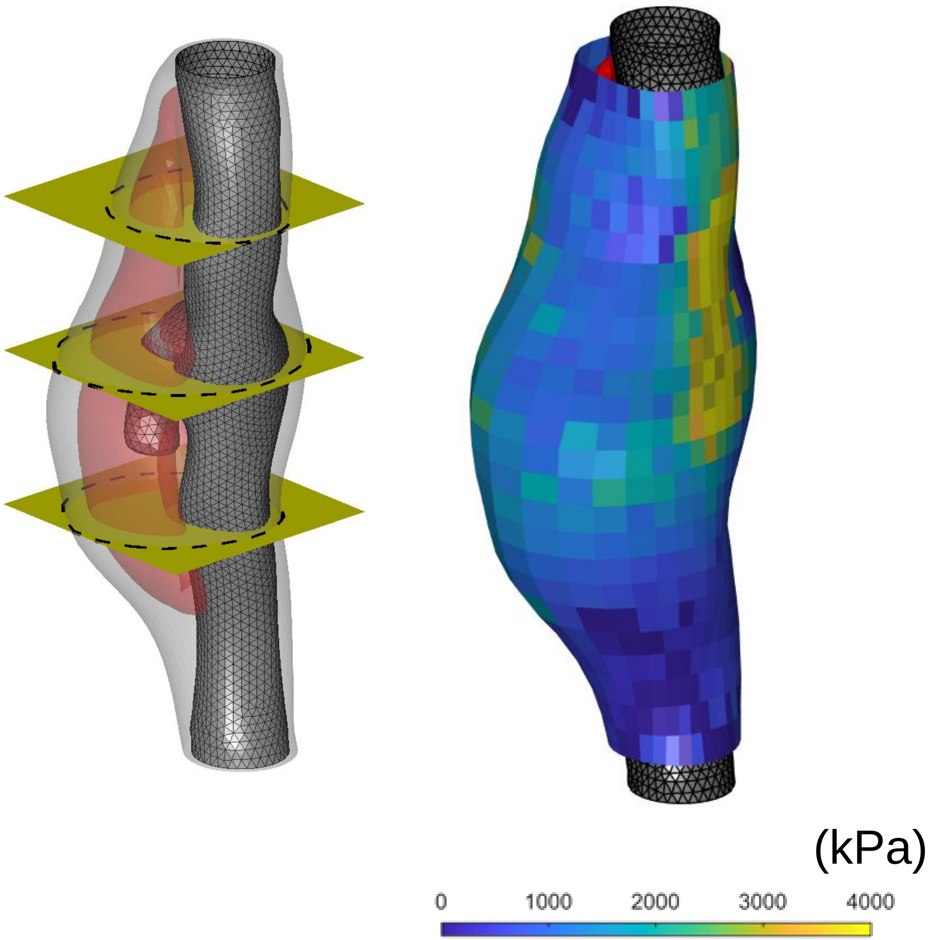

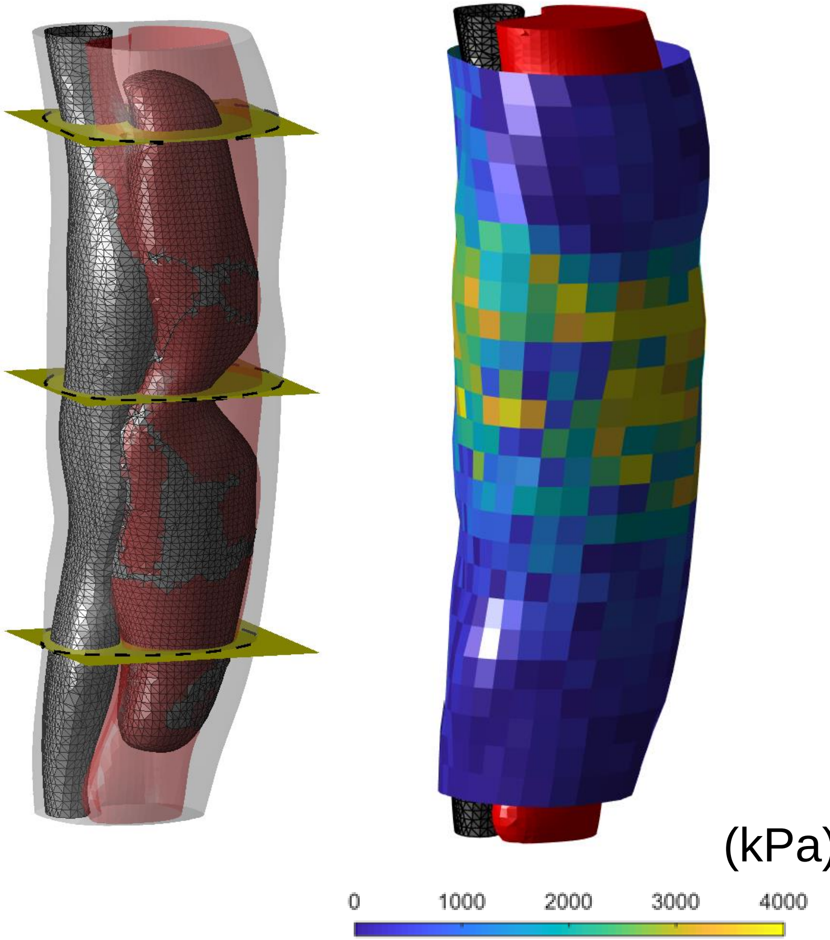

avril@emse.fr

Inverse approach – traditional approach

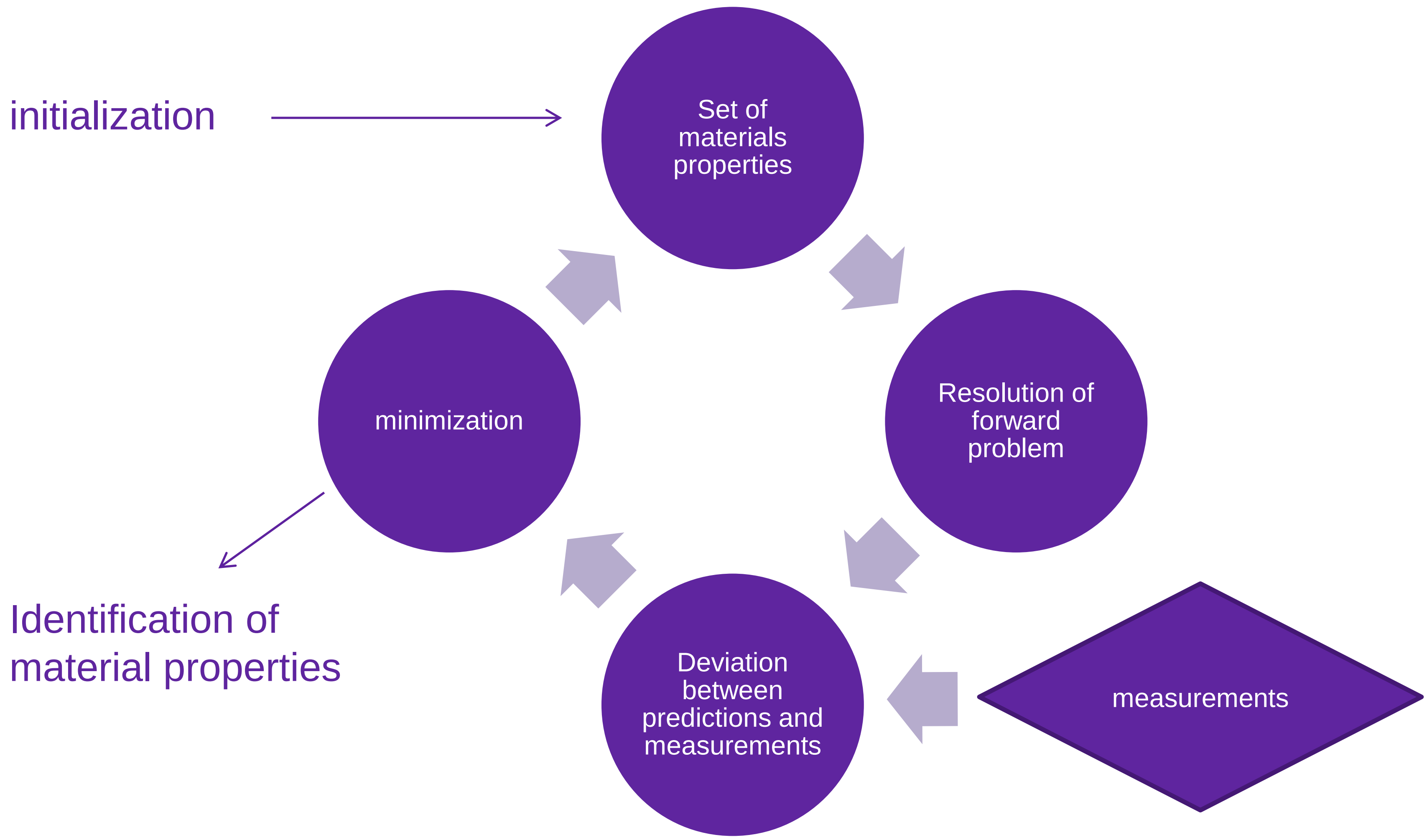

avril@emse.fr

Inverse approach – FEMU approach

initialization

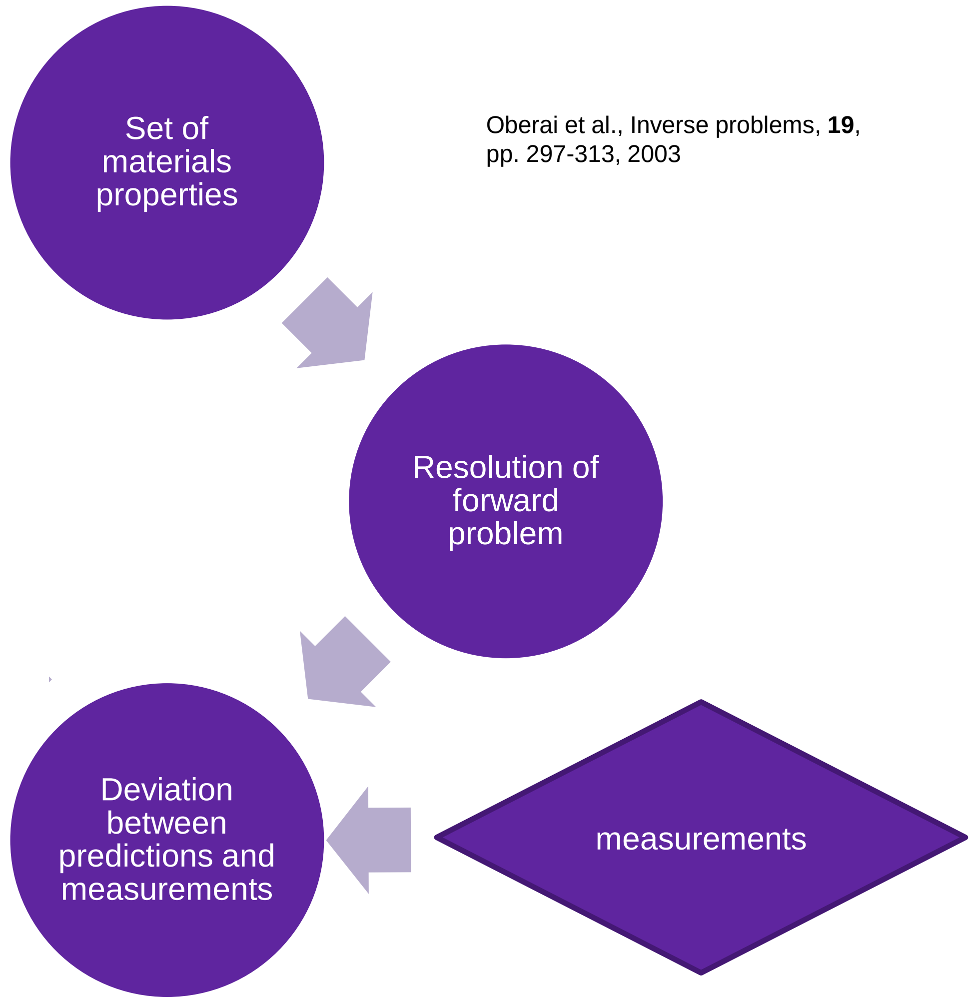

Oberai et al., Inverse problems, **19**, pp. 297-313, 2003

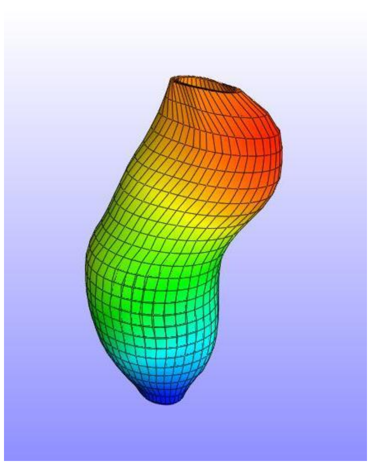

$$J(\mu) = \|T(u) - T(u^{exp})\|^2 + \frac{\alpha}{2} B(\mu)$$

avril@emse.fr

MINES Saint-Étienne

Inverse approach – FEMU approach

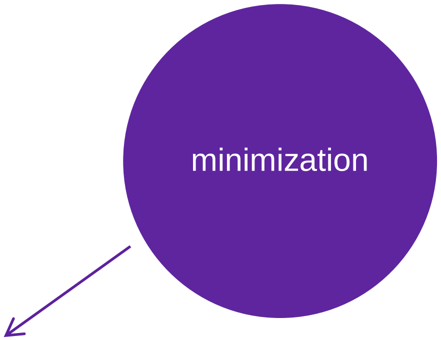

Identification of material properties

1. Use a gradient based method (steepest descent or BFGS)
2. Need to derive the gradient of J with respect to μ at each iteration. With the adjoint method, this requires the resolution of 2 forward problems
3. Very unstable with hyperelastic models: **many risks that the forward problems have a poor convergence**

Alternative inverse approach: the virtual fields method

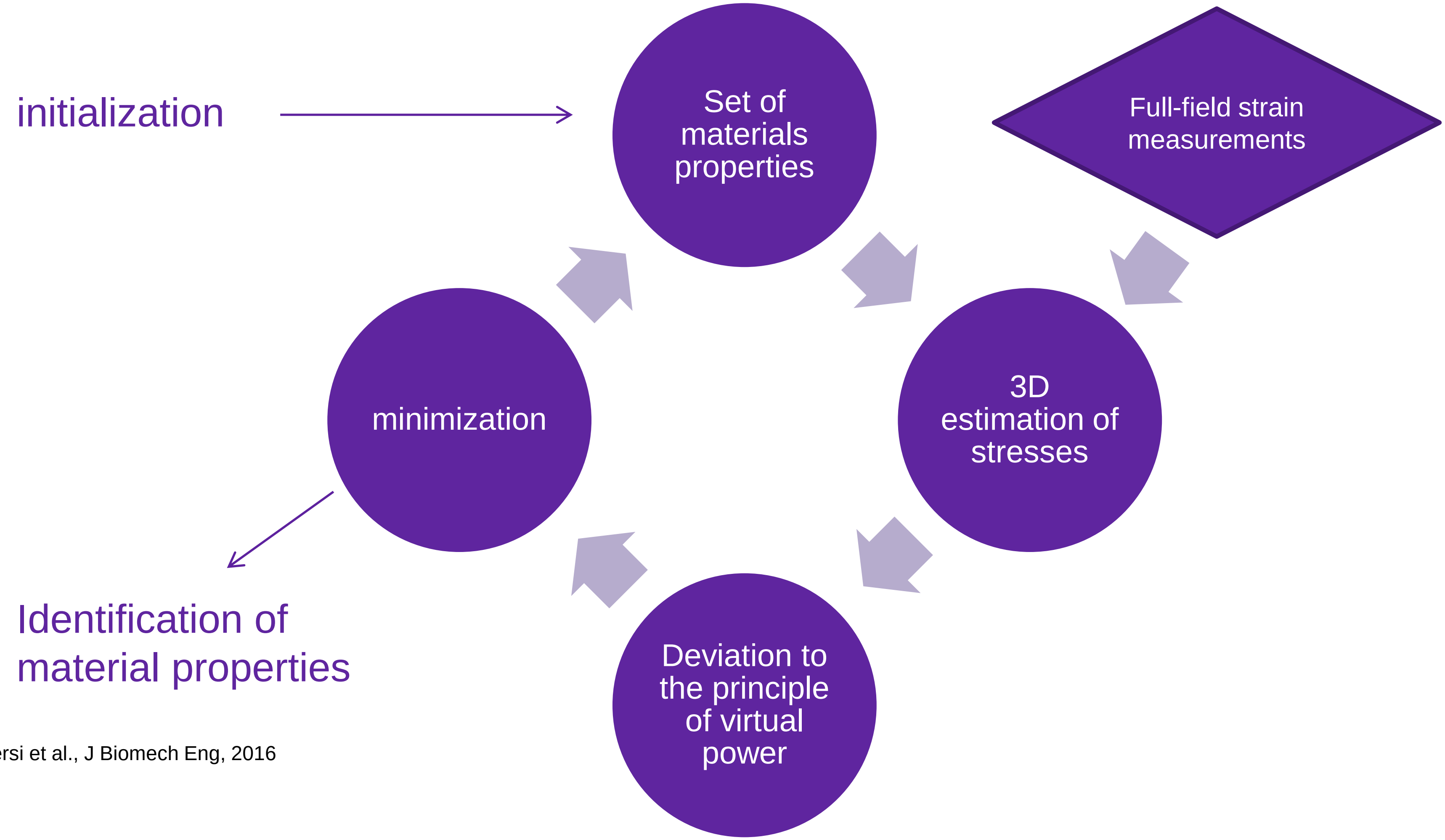

Bersi et al., J Biomech Eng, 2016

Principle of virtual power

$$\int_V \boldsymbol{\sigma} : \mathbf{D}^* dV = \int_V (\mathbf{b} - \mathbf{a}) \cdot \mathbf{v}^* \rho dV + \int_S (\boldsymbol{\sigma} \cdot \mathbf{n_t}) \cdot \mathbf{v}^* dS$$

Internal stresses

Body forces, accelerations

Surface tractions

v* is an arbitrary virtual velocity field

D* is the virtual rate of deformation tensor:

$$\mathbf{D}^* = \frac{1}{2}\left(\nabla \mathbf{v}^* + \nabla^T \mathbf{v}^*\right)$$

avril@emse.fr

The principle of virtual power for incompressible hyperelastic materials

$$\underline{\underline{\sigma}} = \rho \underline{\underline{F}} . \frac{\partial \Psi}{\partial \underline{\underline{E}}} . {}^{t}\underline{\underline{F}} + c \underline{\underline{I}}$$

$$-\int_{V} \left(\rho \underline{\underline{F}} . \frac{\partial \Psi}{\partial \underline{\underline{E}}} . {}^{t}\underline{\underline{F}} + c \underline{\underline{I}} \right) : \underline{\underline{\varepsilon}}^{*} dV + \int_{\partial V} \underline{T} . \underline{u}^{*} dS = 0$$

Grediac et al, Strain 42 (4), 233-253

avril@emse.fr

MINES Saint-Étienne

Application to the NeoHookean incompressible model

$$\underline{\underline{\sigma}} = 2C_{10}\,\underline{\underline{F}}.{}^t\underline{\underline{F}} + c\underline{\underline{I}}$$

$$2C_{10}\int_V \left(\underline{\underline{F}}.{}^t\underline{\underline{F}} + c\underline{\underline{I}}\right) : \underline{\underline{\varepsilon}}^* dV = \int_{\partial V} \underline{T}.\underline{u}^* dS$$

$$C_{10} = \frac{\int_{\partial V} \underline{T}.\underline{u}^* dS}{2\int_V \left(\underline{\underline{F}}.{}^t\underline{\underline{F}} + c\underline{\underline{I}}\right) : \underline{\underline{\varepsilon}}^* dV} = \frac{\int_{\partial V} \underline{T}.\underline{u}^* dS}{2\int_V \left(\underline{\underline{B}} + c\underline{\underline{I}}\right) : \underline{\underline{\varepsilon}}^* dV}$$

Hyperelasticity of Soft Tissues and Related Inverse Problems. Stéphane Avril, Sam Evans Material Parameter Identification and Inverse Problems in Soft Tissue Biomechanics, 573, Springer, pp.37 - 66, 2016,

Application in simple uniaxial tension

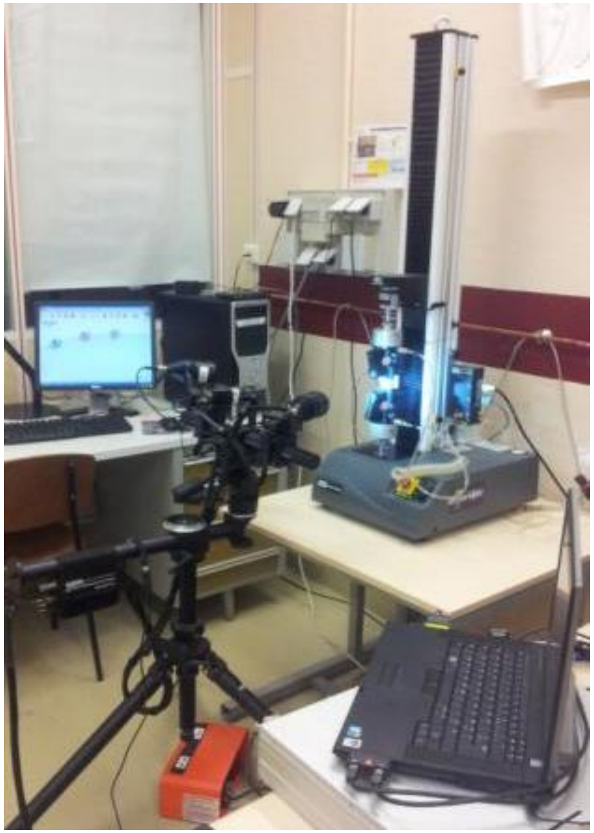

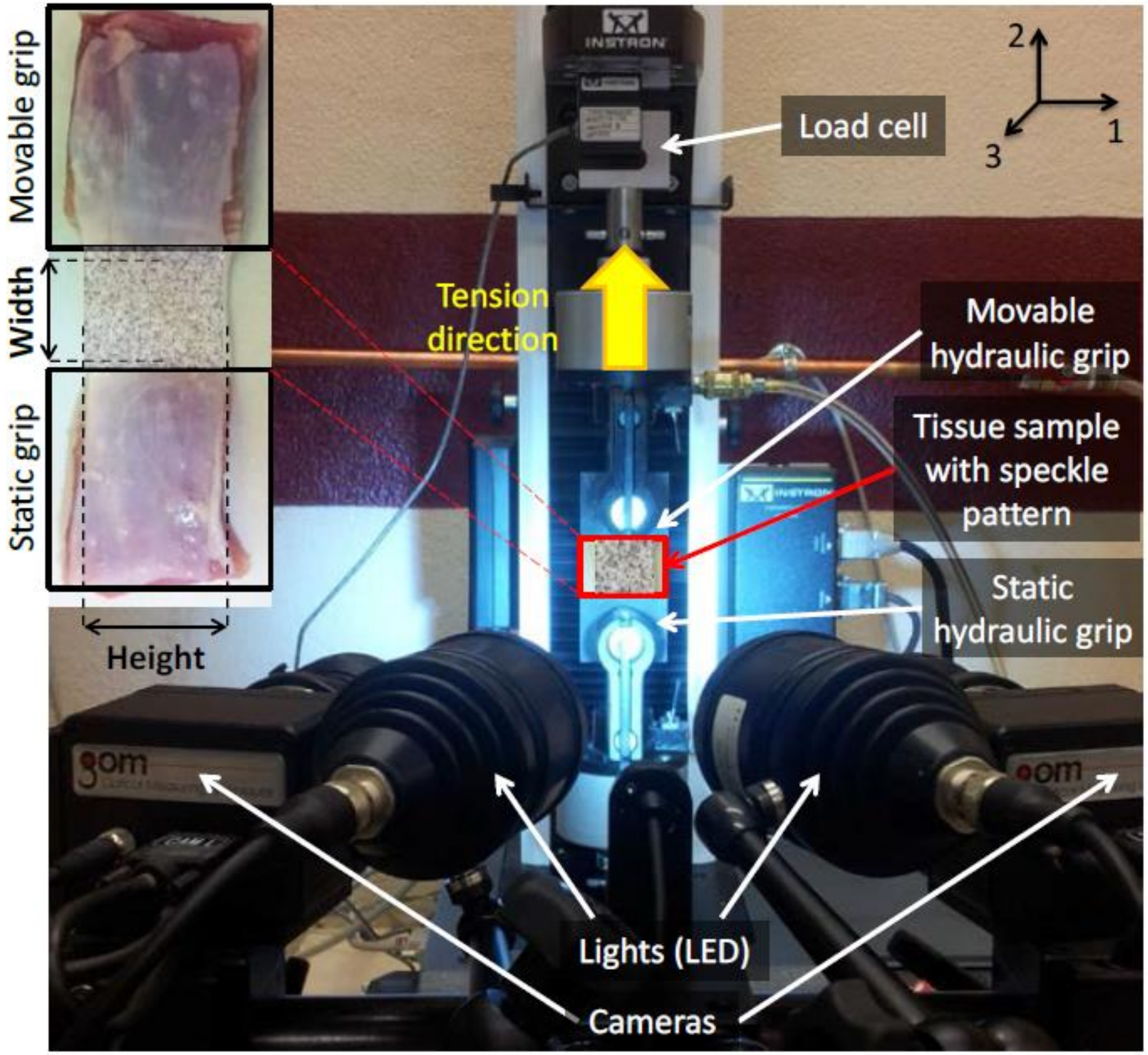

avril@emse.fr

Application in simple uniaxial tension

$$\underline{u}^* = \begin{Bmatrix} x \\ -y/2 \\ -z/2 \end{Bmatrix}$$

$$\int_{\partial V} \underline{T}.\underline{u}^* dS = FL$$

$$C_{10} = \frac{FL}{\int_V (B_{11} - B_{22} - B_{33}) dV}$$

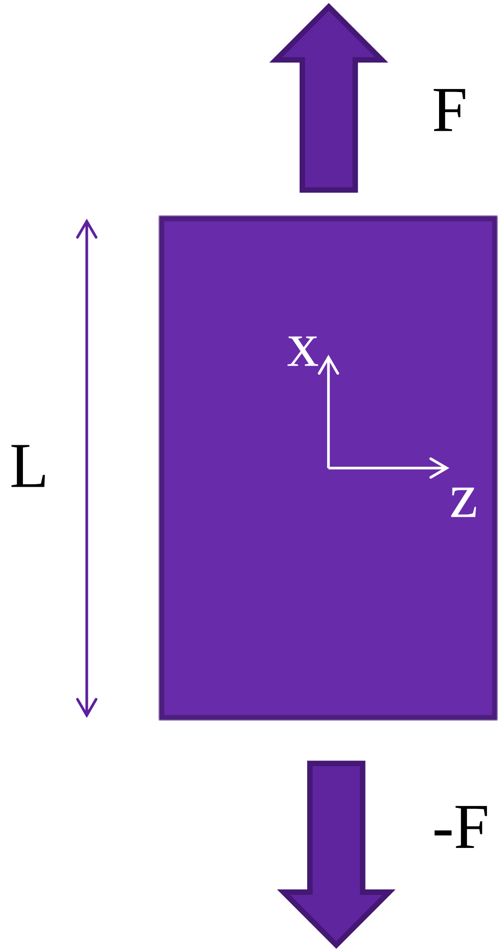

MINES Saint-Étienne

Recent developments and generalized VFM

1. Material property variation

2. New iterative algorithm

3. First applications of the new generalized VFM

avril@emse.fr

Varying the material properties result in variations of stresses

Yue Mei et al, Journal of Elasticity 145 (1), 265-294

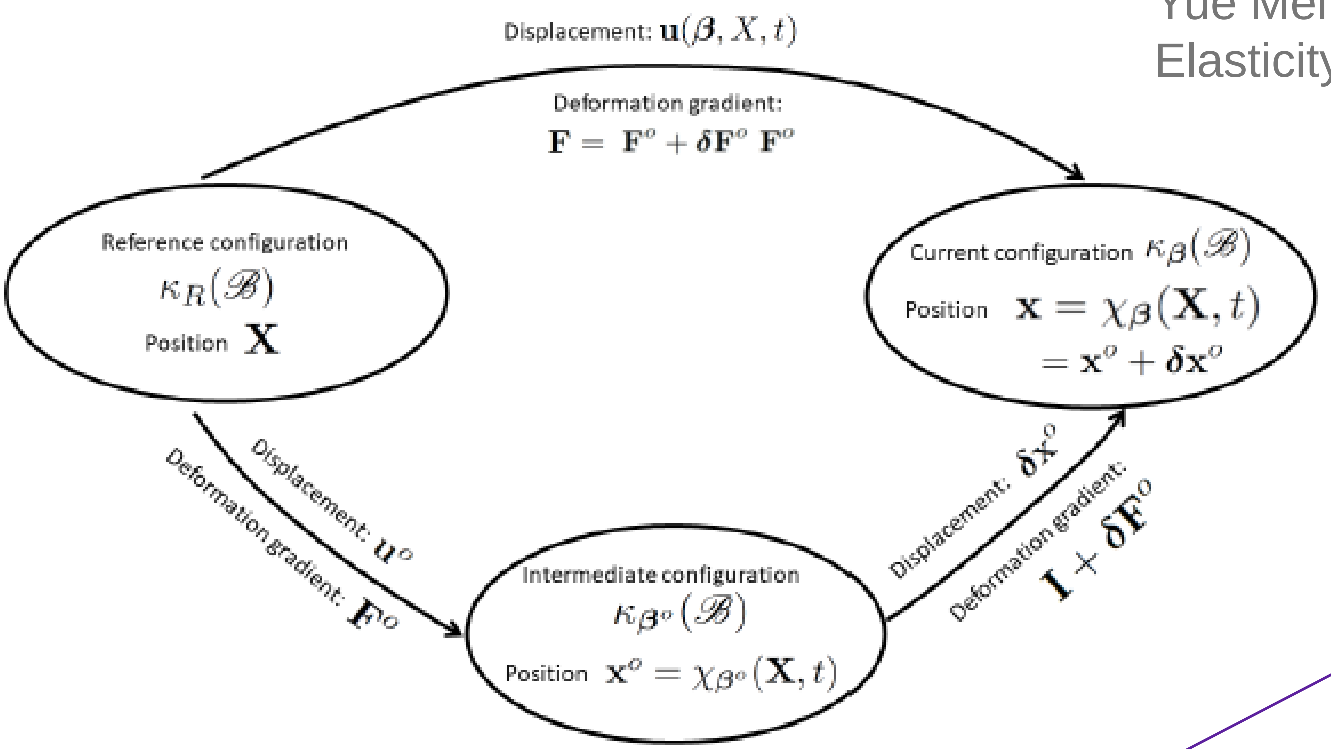

measured

computed

Variations of stresses:

$$\delta \mathbf{T}^o = \mathbb{L}^o : \delta \mathbf{F}^o + \sum_{q=1}^{N} \delta\beta_q\, \mathbf{T}^o_{,\beta_q},$$

avril@emse.fr

MINES Saint-Étienne

Variations of stresses should satisfy the principle of virtual power

$$\int_{\chi_{\beta^o}(\mathscr{B},t)} \delta \mathbf{T}^o : \boldsymbol{\nabla} \delta \mathbf{u}^{o(n)} dV^o = 0 \, ,$$

computed ?

$$\begin{bmatrix} \int_{\chi_{\beta^o}(\mathscr{B})} \mathbf{T}^o_{,\beta_1} : \boldsymbol{\nabla} \delta \mathbf{u}^{o(1)} dV^o & \dots & \int_{\chi_{\beta^o}(\mathscr{B})} \mathbf{T}^o_{,\beta_N} : \boldsymbol{\nabla} \delta \mathbf{u}^{o(1)} dV^o \\ \vdots & \ddots & \vdots \\ \int_{\chi_{\beta^o}(\mathscr{B})} \mathbf{T}^o_{,\beta_1} : \boldsymbol{\nabla} \delta \mathbf{u}^{o(N)} dV^o & \dots & \int_{\chi_{\beta^o}(\mathscr{B})} \mathbf{T}^o_{,\beta_N} : \boldsymbol{\nabla} \delta \mathbf{u}^{o(N)} dV^o \end{bmatrix}$$

$$\times \begin{pmatrix} \delta \beta^o_1 \\ \vdots \\ \delta \beta^o_N \end{pmatrix} = - \begin{pmatrix} \int_{\chi_{\beta^o}(\mathscr{B})} \tilde{\mathbf{H}} : \left(\mathbb{L}^{oT} : \boldsymbol{\nabla} \delta \mathbf{u}^{o(1)} \right) dV^o \\ \vdots \\ \int_{\chi_{\beta^o}(\mathscr{B})} \tilde{\mathbf{H}} : \left(\mathbb{L}^{oT} : \boldsymbol{\nabla} \delta \mathbf{u}^{o(N)} \right) dV^o \end{pmatrix} ,$$

measured computed

Variations of stresses should satisfy the principle of virtual power

Spatial form

$$\begin{bmatrix} \int_{\chi_{\beta^o}(\mathscr{B})} \mathbf{T}^o_{,\beta_1} : \nabla\mathfrak{L}(\mathbf{T}^o_{,\beta_1}) dV^o & \dots & \int_{\chi_{\beta^o}(\mathscr{B})} \mathbf{T}^o_{,\beta_N} : \nabla\mathfrak{L}(\mathbf{T}^o_{,\beta_1}) dV^o \\ \vdots & \ddots & \vdots \\ \int_{\chi_{\beta^o}(\mathscr{B})} \mathbf{T}^o_{,\beta_1} : \nabla\mathfrak{L}(\mathbf{T}^o_{,\beta_N}) dV^o & \dots & \int_{\chi_{\beta^o}(\mathscr{B})} \mathbf{T}^o_{,\beta_N} : \nabla\mathfrak{L}(\mathbf{T}^o_{,\beta_N}) dV^o \end{bmatrix} \times \begin{pmatrix} \delta\beta^o_1 \\ \delta\beta^o_2 \\ \vdots \\ \delta\beta^o_N \end{pmatrix} = - \begin{pmatrix} \int_{\chi_{\beta^o}(\mathscr{B})} \tilde{\mathbf{H}} : \mathbf{T}^o_{,\beta_1} dV^o \\ \vdots \\ \int_{\chi_{\beta^o}(\mathscr{B})} \tilde{\mathbf{H}} : \mathbf{T}^o_{,\beta_N} dV^o \end{pmatrix} . \quad (44)$$

computed

measured

computed

avril@emse.fr

MINES Saint-Étienne

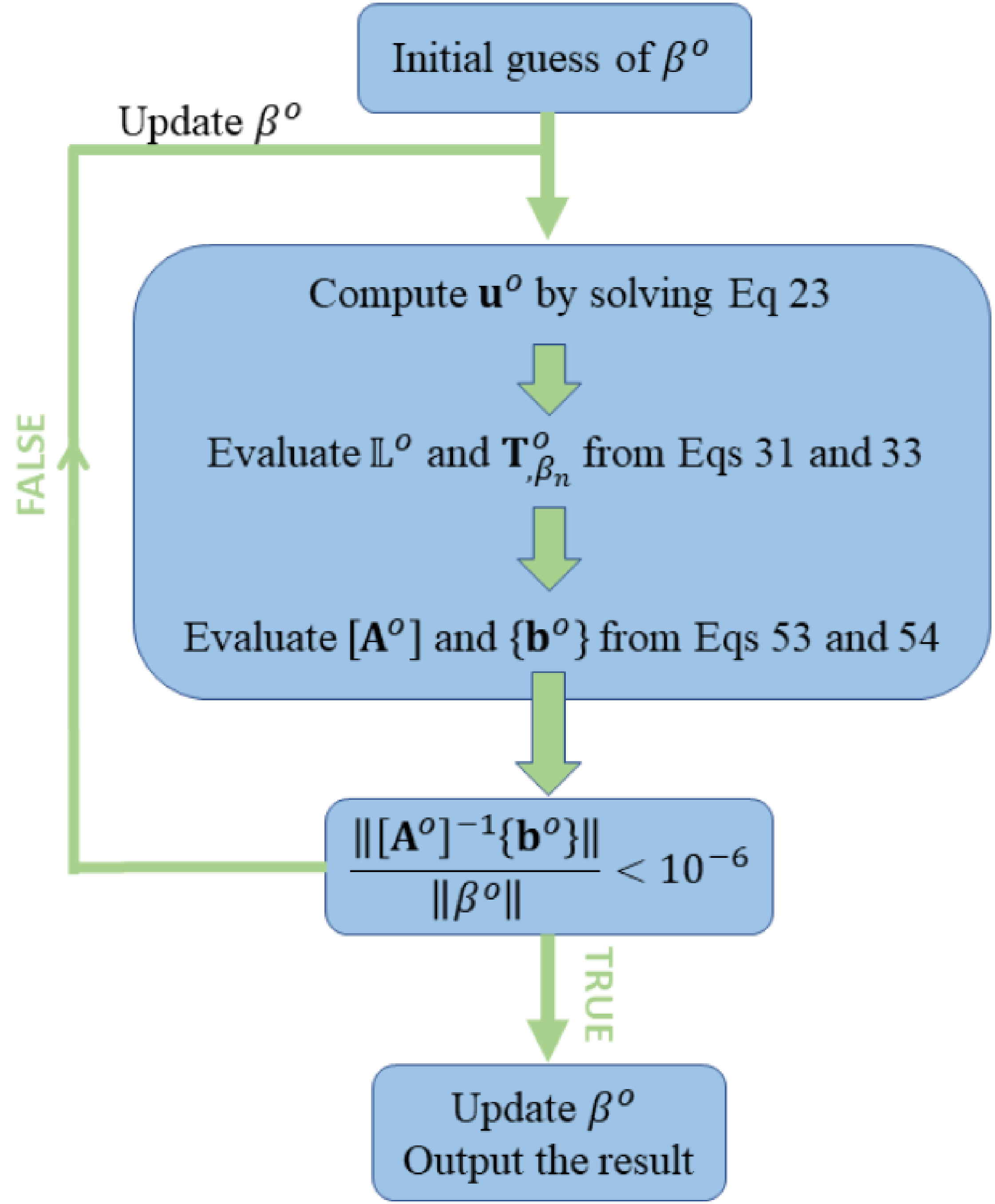
Initial guess of β^o
Update β^o
FALSE
Compute $\mathbf{u}^o$ by solving Eq 23
Evaluate $\mathbb{L}^o$ and $\mathbf{T}^o_{,\beta_n}$ from Eqs 31 and 33
Evaluate $[\mathbf{A}^o]$ and $\{\mathbf{b}^o\}$ from Eqs 53 and 54
$\frac{\|[\mathbf{A}^o]^{-1}\{\mathbf{b}^o\}\|}{\|\beta^o\|} < 10^{-6}$
TRUE
Update β^o
Output the result

Quadratic convergence / recent progress

Yue Mei et al, Journal of Elasticity 145 (1), 265-294

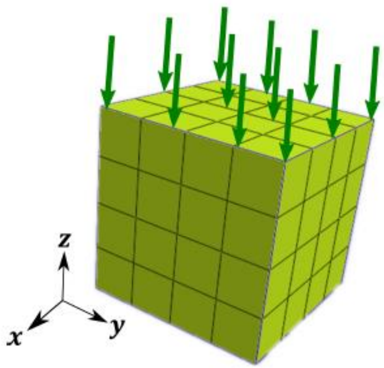

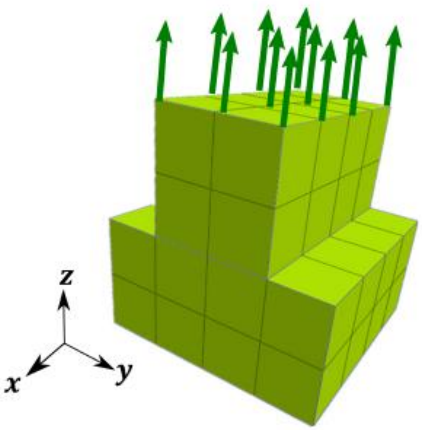

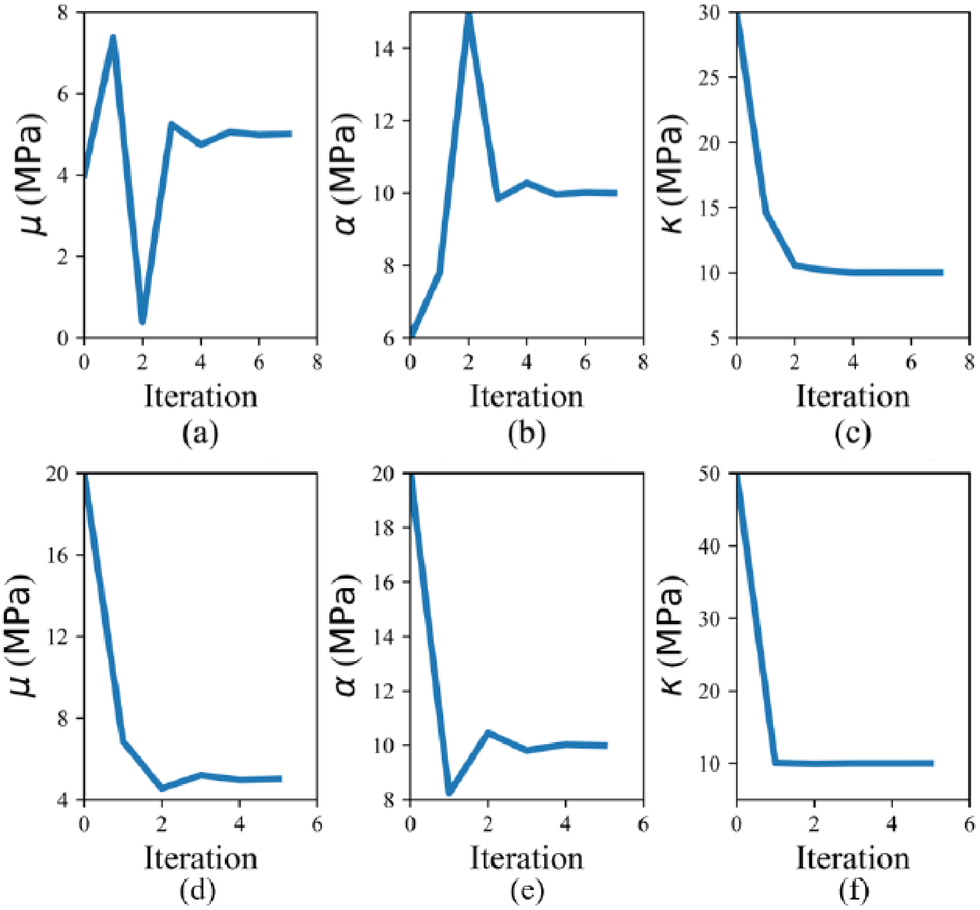

avril@emse.fr

MINES Saint-Étienne

Specific problem of the optical nerve head

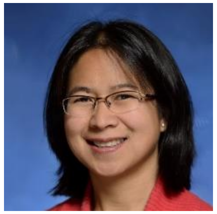

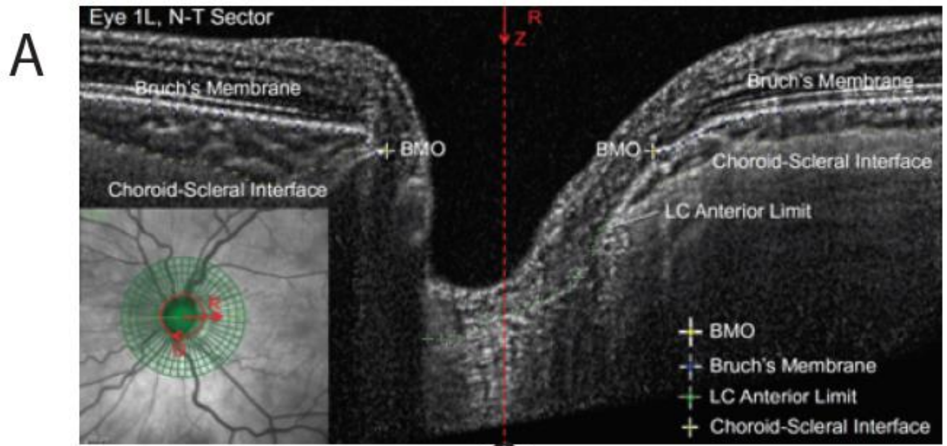

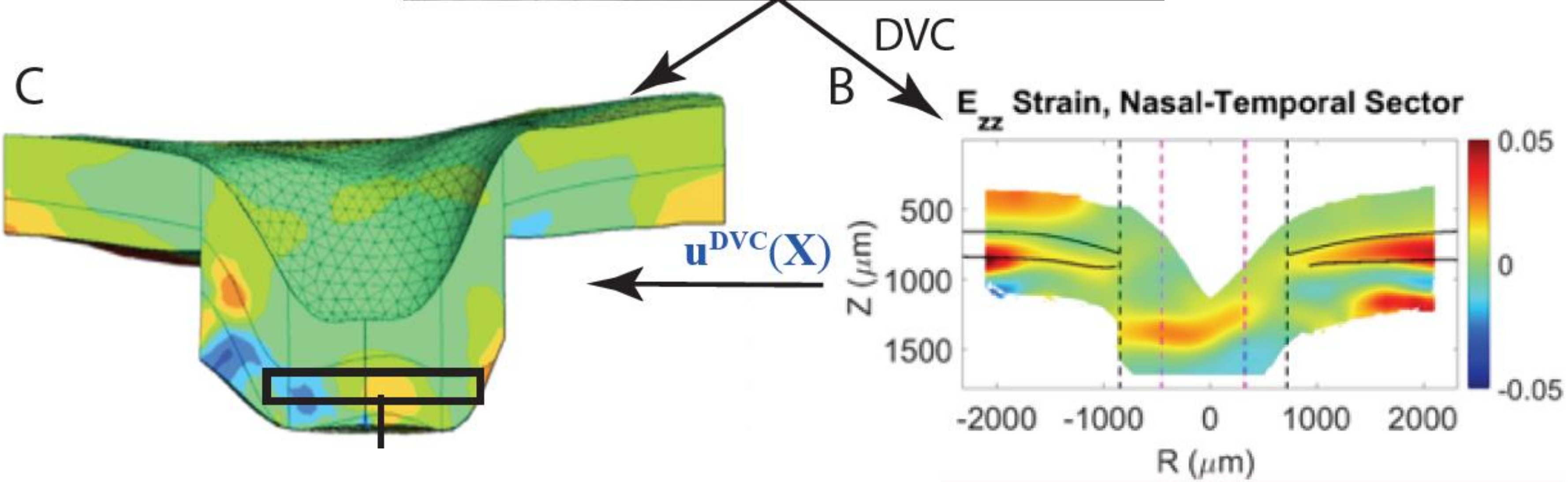

in vivo OCT

avril@emse.fr

Application to the eye problem

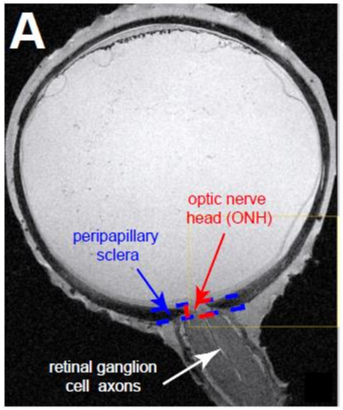

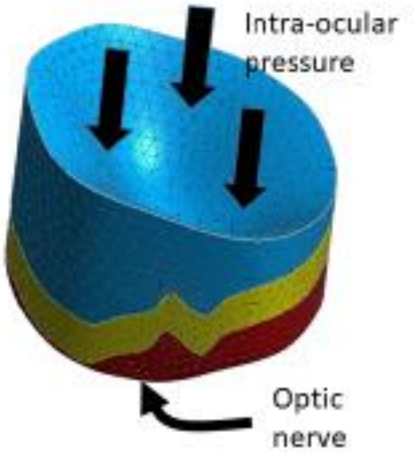

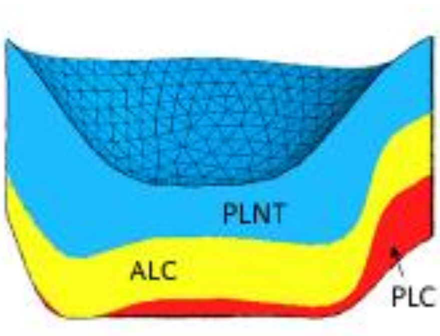

	Reference κ	Identified κ after 4 iterations	relative error	Identified κ after 5 iterations	relative error
PLNT	2.29 MPa	2.31 MPa	0.82%	2.284 MPa	0.35%
ALC	2.5 MPa	2.51 MPa	0.55%	2.495 MPa	0.22%
PLC	2.71 MPa	2.72 MPa	0.37%	2.706 MPa	0.08%

Yue Mei et al, Journal of Elasticity 145 (1), 265-294

New applications in progress

1. Eardrum and other membrane inflation

2. Elastography

3. Biphasic behavior / osmotic effects

4. Brain shift

avril@emse.fr

Eardrum and other membrane inflation

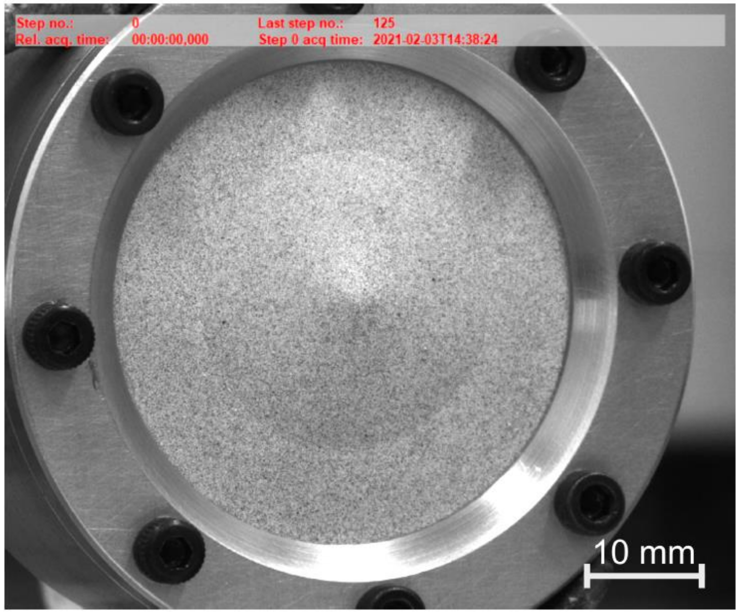

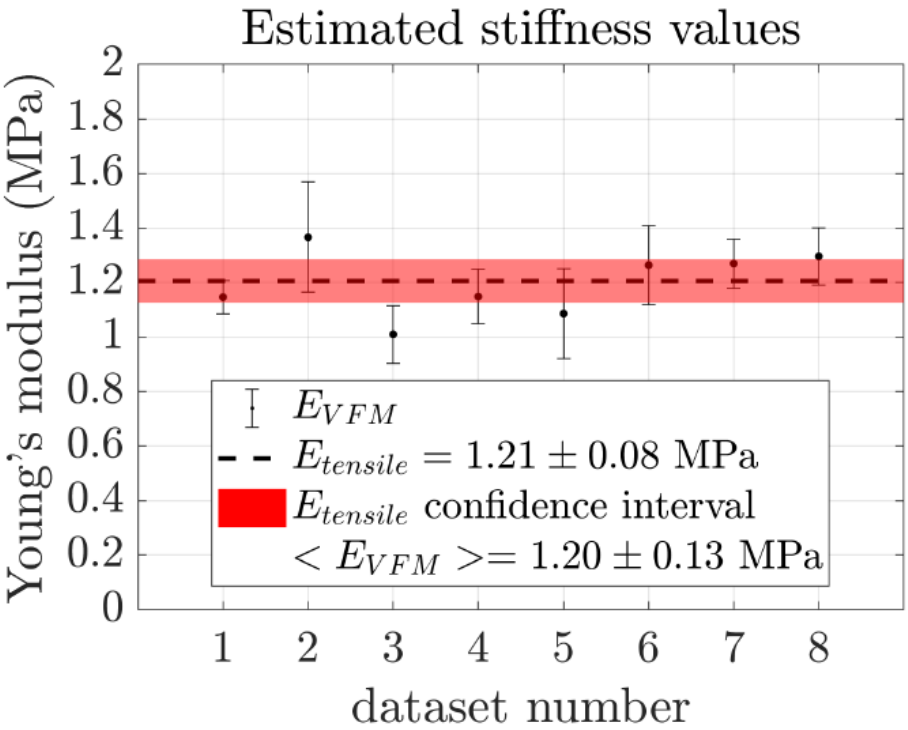

Rubber membrane

Livens et al, Strain 57 (6), e12398

Elastography

Computational Mechanics 67 (6), 1581-1599

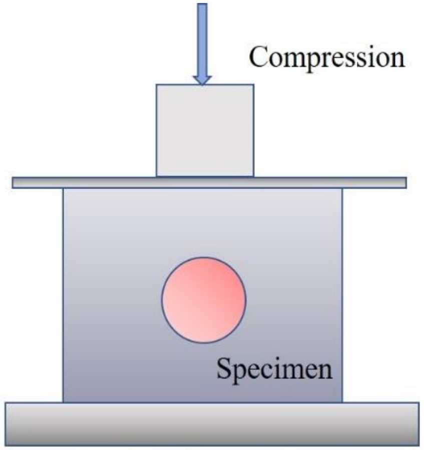

(a) Experiment setup

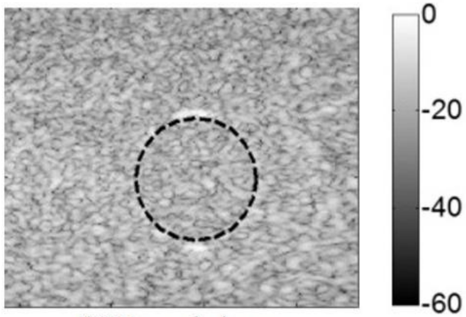

(b) B-mode image

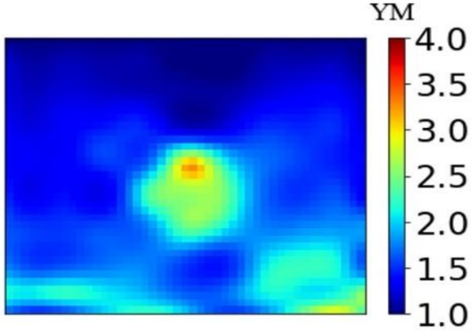

Biphasic behavior : osmotic effects

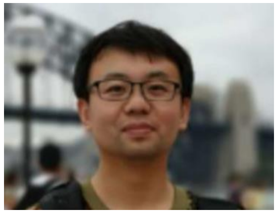

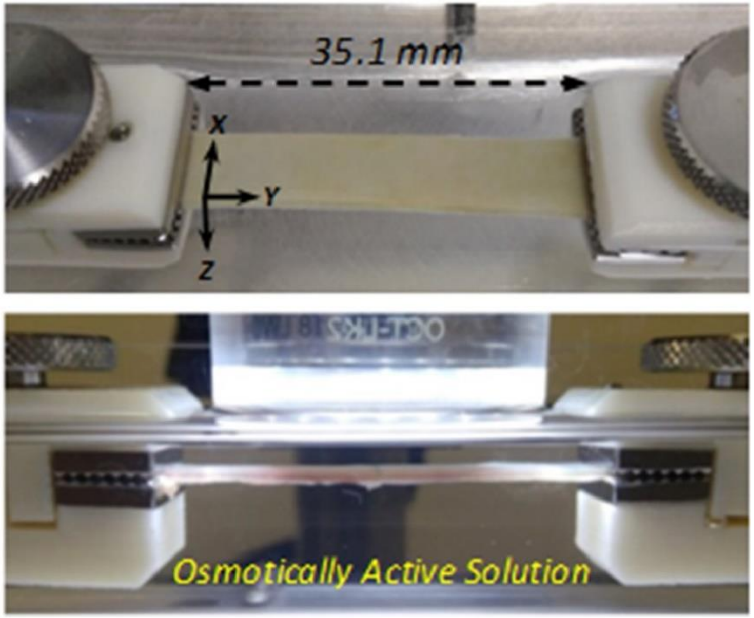

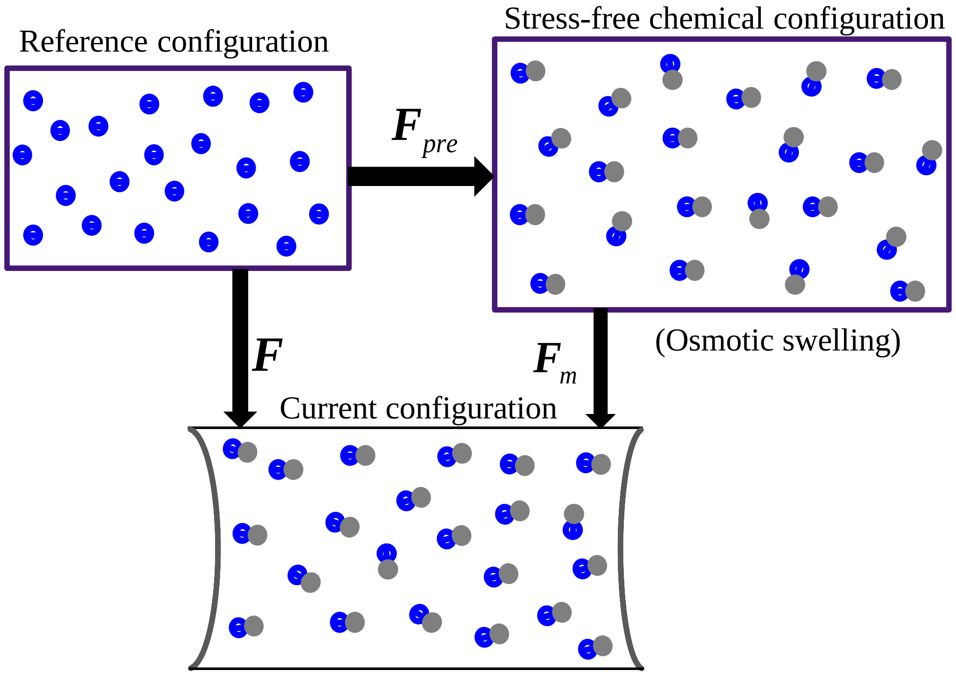

$$\boldsymbol{T}_i = -P\boldsymbol{I} = -R\theta[\sqrt{(\mathrm{c}^{\mathrm{F}})^2 + (\bar{\mathrm{c}}^*)^2} - \bar{\mathrm{c}}^*]\boldsymbol{I}$$

$$\boldsymbol{T} = \boldsymbol{T}_i + \boldsymbol{T}_s$$

- $\boldsymbol{T}_s = \mu_0 J^{-\frac{5}{3}}\left(\boldsymbol{B} - \frac{1}{3}I_1\boldsymbol{I}\right) + \kappa_0(J-1)\boldsymbol{I}$

avril@emse.fr

MINES Saint-Étienne

Brain shift

$$\int_V \boldsymbol{\sigma} : \mathbf{D}^* dV = \int_V (\mathbf{b} - \mathbf{a}) \cdot \mathbf{v}^* \rho dV + \int_S (\boldsymbol{\sigma} \cdot \mathbf{n_t}) \cdot \mathbf{v}^* dS$$

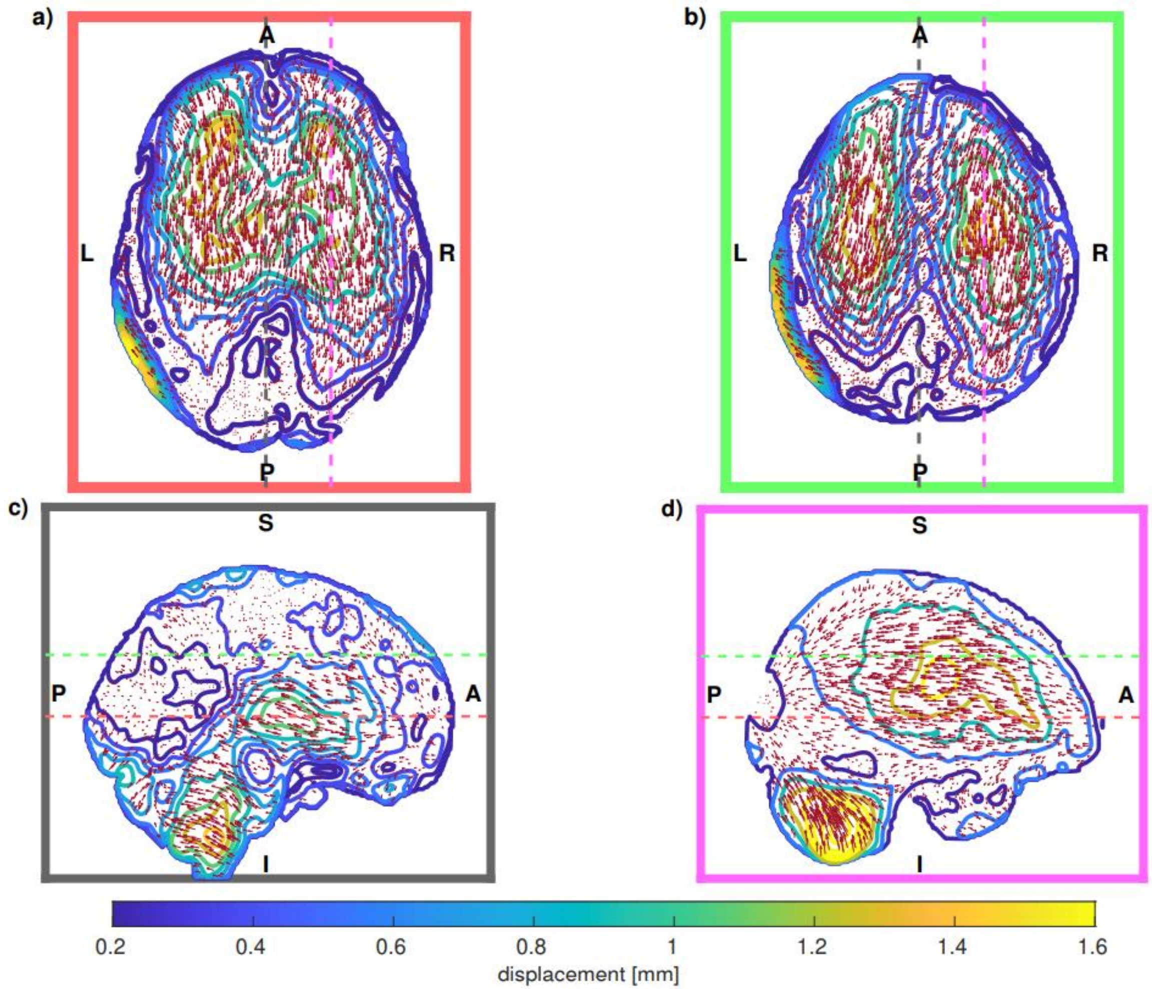

Acknowledgements

国家自然科学基金委员会
National Natural Science Foundation of China

erc
European Research Council
Established by the European Commission
© ERC

European Commission
HORIZON 2020

avril@emse.fr

MINES
Saint-Étienne